Inorganic Chemistry

Article

pubs.acs.org/IC

First-Principles Prediction of New Complex Transition Metal Hydrides for High Temperature Applications

Kelly M. Nicholson and David S. Sholl*

School of Chemical & Biomolecular Engineering, Georgia Institute of Technology, 311 Ferst Drive, Atlanta, Georgia 30332-0100, United States

Supporting Information

ABSTRACT: Metal hydrides with high thermodynamic stability are desirable for high-temperature applications, such as those that require high hydrogen release temperatures or low hydrogen overpressures. First-principles calculations have been used previously to identify complex transition metal hydrides (CTMHs) for high temperature use by screening materials with experimentally known structures. Here, we extend our previous screening of CTMHs with a library of 149 proposed materials based on known prototype structures and charge balancing rules. These proposed materials are typically related to known materials by cation substitution. Our semiautomated, high-throughput screening uses density functional theory (DFT) and grand canonical linear programming (GCLP) methods to compute thermodynamic properties and phase diagrams: 81 of the 149 materials are found to be thermodynamically stable. We identified seven proposed materials that release hydrogen at higher temperatures than the associated binary hydrides and at high temperature, $T > 1000$ K, for 1 bar H_2 overpressure. Our results indicate that there are many novel CTMH compounds that are thermodynamically stable, and the computed thermodynamic data and phase diagrams should be useful for selecting materials and operating parameters for high temperature metal hydride applications.

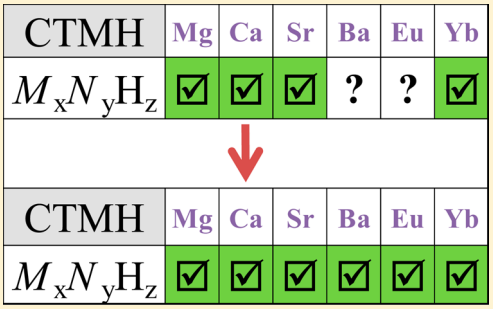

INTRODUCTION

In their comprehensive 2005 review, Yvon and Renaudin described 127 ternary and quaternary complex transition metal hydrides (CTMHs) that crystallize in 47 structure prototypes, compared with just 13 prototypes in 1991.[1] Among those listed are Mg_2FeH_6, which has the highest known hydrogen density by volume at 120 g H_2 L^{-1}, $BaReH_9$ with a higher hydrogen concentration on an atom basis than methane, and Mg_2NiH_4, which undergoes a metal to nonmetal transition upon hydrogenation that may be useful for applications such as switchable mirrors.[1,2] A convenient measure of thermodynamic stability of these materials is the decomposition temperature, T_d, at which a metal hydride is in thermodynamic equilibrium with $P = 1$ bar H_2. If heated to temperatures above T_d, the hydride will release hydrogen. Since most CTMHs have T_d values greater than 550 K and large enthalpies of formation, $\Delta H > 80$ kJ mol^{-1} H_2, they have largely been ignored for ambient temperature applications such as the onboard solid state storage of hydrogen in fuel cell vehicles.[1,3] However, their high stabilities and hydrogen capacities make them potentially attractive for high-temperature applications, such as the thermochemical storage of heat for solar thermal plants for which hydrogen discharge temperatures exceeding 700 K are desired[4−7] or for use as tritium (^3H) gettering materials in the U.S. Department of Energy Next Generation Nuclear Plant (NGNP).[8−12] In the proposed NGNP, helium coolant will exit a very high temperature gas-cooled reactor at temperatures in the range $1000 < T$ (K) < 1200 and could be used to provide high temperature process heat to industrial users if the trace tritium contaminant can be removed, for example, via highly stable metal hydrides.

Recently, we performed a large scale computational screening study based on density functional theory (DFT) and grand canonical linear programming (GCLP) phase diagram prediction of over 100 known, "simulation ready" CTMHs for high temperature metal hydride applications and identified 13 candidates with the desirable properties of enhanced stability relative to the parent binary hydrides ($T_d/T_{d,binary} > 1$) and high hydrogen release temperature ($T_d > 1000$ K).[3] Enhanced stability relative to the parent binary hydrides, M_xH_y (M = metal), ensures that the ternary or higher hydride defines the most stable hydride phase in the element space, that is, higher operating temperatures can be reached through use of a multimetal hydride than with a binary hydride alone. In this paper, we greatly extend the set of known CTMHs via first-principles structure prediction. By examining structures that can be related to existing materials by cation substitution, we consider 149 previously unstudied CTMHs. For each material, we assess thermodynamic stability with respect to our previously developed library of CTMHs. Together with the screening of known compounds, these results present thermodynamic information for the most stable CTMHs and provide a guide for selecting materials for high temperature or

Received: August 15, 2014
Published: October 31, 2014

   dx.doi.org/10.1021/ic501992x | Inorg. Chem. 2014, 53, 11849−11860

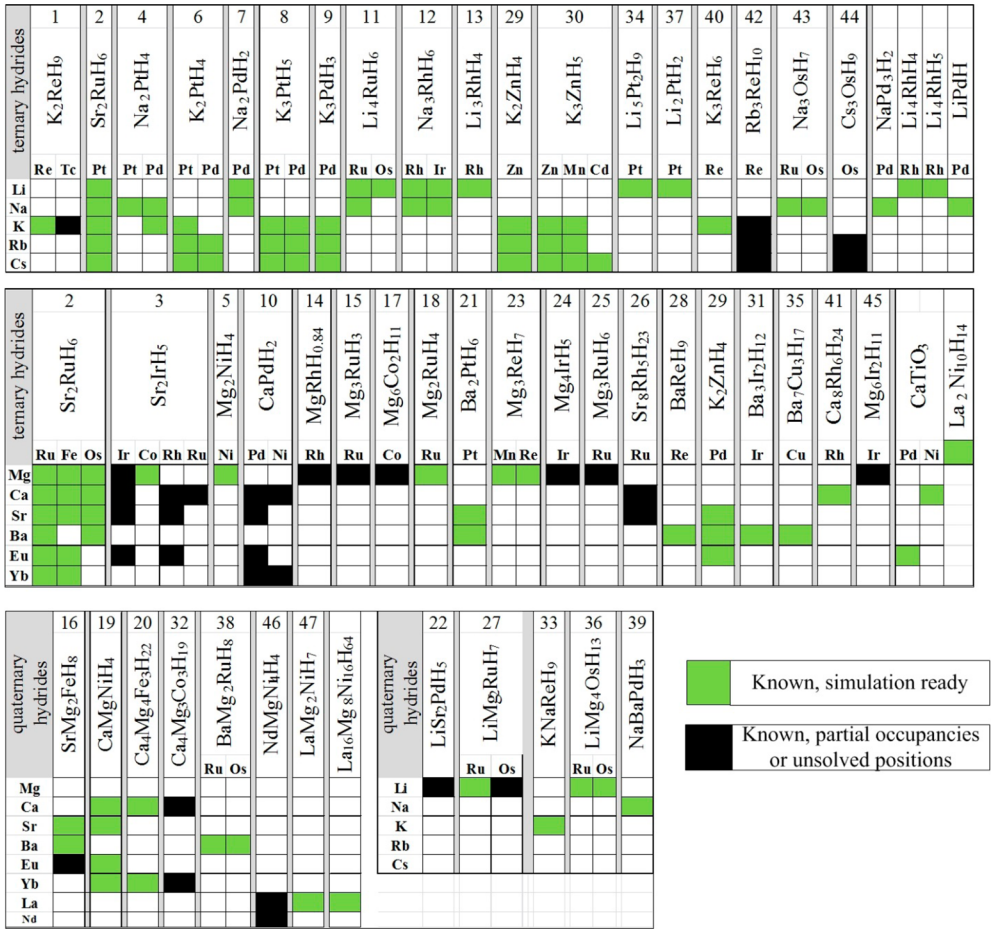

Figure 1. Experimentally known ternary ($M-Tr-$H) and quaternary (M_1-M_2-Tr-H) complex transition metal hydrides from the ICSD[14,15] and the Yvon and Renaudin 2005 Review.[1] Numbers are consistent with Yvon and Renaudin[1] and describe the chronological discovery of the prototype ternary hydride M_x Tr_y H_z crystal structure shown vertically. Substitutional cations M of the same valence are grouped vertically. Substitutional transition metals Tr are listed horizontally. Simulation ready implies completely solved and ordered structure with no partial occupancies. Reproduced from ref 3. Copyright 2014 American Chemical Society.

low hydrogen pressure applications such as the NGNP. Additionally, we identify many hypothetical CTMHs that are predicted to be thermodynamically stable.

CTMHs are inorganic compounds that are stabilized via charge transfer from a monovalent, divalent, or trivalent cation, M (typically an alkali, alkaline earth, or lanthanide species), to an anionic transition metal hydrido complex, $[TrH_n]$. Known transition metal hydrido complexes form from late 3d, 4d, and 5d transition metals of groups 7−10. Currently, no known complexes have been identified experimentally for elements of groups 4−6 or the elements Ag, Au, or Hg.[1,13] Compounds can be divided into two broad classifications that describe the hydrogen bonding schemes: $M_m^{\delta+}$ $[TrH_n]^{\delta-}$ (m, n, δ = 1, 2, 3, ...) and $M_m^{\delta+}$ $[TrH_n]^{\delta-}$ $M_o^{\delta+}$ H_p^- (m, n, o, p, δ = 1, 2, 3, ...). In the former, hydrogen is covalently bound to the transition metal, and in the latter composite-type hydride, hydrogen is covalently bound to the transition metal and also available in interstitial sites as anions that interact directly with the cations. Figure 1 maps the series of known ternary and quaternary CTMHs based on both the 2005 Yvon and Renaudin review[1] and a survey of the ICSD[14,15] for stoichiometric compounds with compositions similar to the known CTMHs. Alkali, alkaline earth, and lanthanide species are arranged vertically, and the prototype structures with transition metal substitutions follow horizontally. The prototype numbering system describes the chronological order in which a prototype was experimentally identified based on the Yvon and Renaudin review.[1] Prototypes without a numeral were retrieved from the ICSD and do not appear in the review. More information on the compilation of this figure is available in ref 3. Stable compounds tend to form in a given prototype down a group with cations of the same valence, thus maintaining charge neutrality. For example, 2−$M_2[RuH_6]^{4-}$ (the Sr_2RuH_6 prototype where 2 is the numeral identifier from Figure 1) forms compounds for M^{2+} = Mg, Ca, Ba, Sr, Eu, and Yb. Similarly, materials have been identified for 2−$M_2[FeH_6]^{4-}$ (M^{2+} = Mg, Ca, Sr, Eu, and Yb). There is, however, no known compound that forms with the composition Ba_2FeH_6 in this prototype. Additionally, there are no ICSD entries for Eu_2OsH_6 or Yb_2OsH_6 in the 2−Sr_2RuH_6 prototype structure (or in any other crystal structure). Currently, we have no indication as to whether or not synthesis of these compounds has ever been attempted, although as recently as 2010, Li_2PtH_6 was synthesized at high H_2 pressures in the 2−Sr_2RuH_6 prototype to complete the series of alkali metals.[16]

In this Article, we perform DFT calculations to first predict if the 149 "missing" ternary compounds shown in Figure 2 are thermodynamically viable based on ground state energies with respect to our DFT materials library from Table S.1 of ref 3, which contains over 260 known simulation ready compounds.

dx.doi.org/10.1021/ic501992x | Inorg. Chem. 2014, 53, 11849−11860

Figure 2. Mapping of 149 proposed and experimentally known ternary (M−Tr−H) CTMHs studied with DFT and screened for enhanced thermodynamic properties. Known CTMHs are from the Yvon and Renaudin 2005 Review[1] and the ICSD.[14,15] Numbers are consistent with Yvon and Renaudin[1] and describe the chronological discovery of the prototype ternary hydride M_x Tr_y H_z crystal structure shown vertically. Substitutional cations M of the same valence are grouped vertically. Substitutional transition metals Tr are listed horizontally. Simulation ready implies completely solved and ordered structure with no partial occupancies.

Simulation ready implies that crystal structures are fully ordered with all atomic positions resolved and no partial occupancies. We then subject the predicted stable materials to the same screening procedure used for the known materials, described in ref 3., to identify candidates with both enhanced stability relative to the parent binary hydrides ($T_d/T_{d,binary}$ >1) and high hydrogen release temperature (T_d > 1000 K) for the NGNP and other high temperature applications. Critically, our methods utilize two levels of theory to screen compounds, as discussed in detail in ref 3. In the first round, vibrational contributions to the free energy for the solid compounds are neglected, allowing us to utilize computationally inexpensive DFT ground state energies to retrieve estimates of the relative stabilities of the solid phases. In this approximation, temperature effects are assumed to be controlled through the chemical potential of hydrogen gas. In the second round, more computationally intensive calculations are performed for a smaller selection of compounds to compute the vibrational density of states (VDOS) and, thus, the temperature-dependent vibrational contribution to the Helmholtz free energy of the solid phases. We refer to these calculations as phonon calculations below for brevity. This provides our best estimate of the temperature-dependent relative phase stabilities of the CTMHs and related compounds as given by the phase diagrams.

The proposed materials we test include only those materials for which there are available template materials that are simulation ready. For example we exclude proposed materials such as $SrNiH_2$ that might form in the 10−$CaPdH_2$ prototype or Ca_3RuH_3 in the 15−Mg_3RuH_3 structures because of the presence of partial occupancies on the H sites. These proposed materials require special and individualized treatment, outside of the scope of this large scale screening study. We exclude LiPdH and Li_4RhH_5 templates for this study since these were not found to be thermodynamically stable for any T based on our initial screening of existing CTMHs.[3] We also do not consider quaternary hydrides since we found that quaternary hydrides tend to decompose to mixtures of lower hydrides upon heating in our previous work.[3] Our calculations greatly extend the range of element spaces probed to identify ternary hydrides for the NGNP and other high temperature applications, covering 71 element spaces not previously examined in the screening of known materials, as shown in Figure 3.

COMPUTATIONAL METHODS

Screening Algorithm. First, we relax 149 proposed materials using DFT to obtain ground state DFT energies, E_0, and incorporate

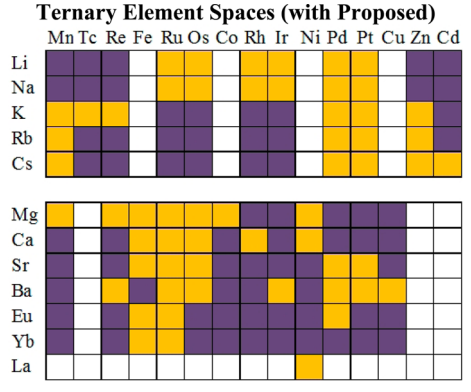

Figure 3. Known (light squares) and proposed (dark squares) ternary M−Tr−H element spaces (element combinations) studied with the round 1 level of screening, based on simulation ready CTMHs from Figure 2. Transition metals, Tr, for ternary spaces are listed horizontally. Alkali and alkaline earth metals are listed vertically. Element combinations not listed or shaded were not included in the overall screening.

dx.doi.org/10.1021/ic501992x | Inorg. Chem. 2014, 53, 11849−11860

the composition and energy into the materials library discussed previously from ref 3. The DFT calculations require an initial crystal structure. Since [TrH_n] complexes behave largely as rigid units, the volume of a CTMH unit cell scales roughly with the ionic radius of the cation. Figure 4 shows relaxed DFT volumes normalized by the ionic

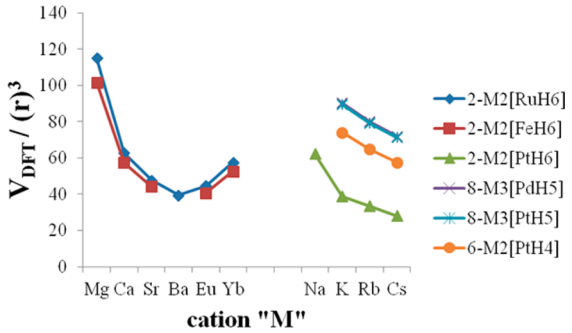

Figure 4. Relationship between cation, *M*, and unit cell volumes of existing CTMHs relaxed using DFT. Volumes are normalized by the ionic radius, *r*, of *M*.[17] Cations are arranged by valence. Numeral identifiers before compositions in legend refer to the prototype structure classification from Figure 1

radius of the cation for a series of prototypes. The relationship is generally smooth, and so we estimate the initial unit cell volume of a given proposed material through simple scaling of the lattice constants of a reference material that crystallizes in the same prototype to account for the ionic radius of the target material.[17] *M* = Ba is missing from the 2−M_2[FeH_6] series of existing materials in Figure 4 because there is no known Ba_2FeH_6 compound that crystallizes in the type 2−Sr_2RuH_6 prototype structure.

For round 1 calculations, we predict phase diagrams at P = 1 bar H_2 for $0 \leq T$ (K) ≤ 2000 for the proposed element spaces in Figure 3 using eq 7 from ref 3., ignoring vibrational contributions to the free energies of the solid phases. We retain element spaces for which there is a stable proposed CTMH. Next, we retrieve simulation ready binary intermetallics from the ICSD[14,15] for retained element spaces not previously scrutinized via the initial screening of known materials. We again predict phase diagrams while including relaxed DFT energies for the additional intermetallics. This is to account for proposed CTMHs that are destabilized by binary intermetallic phase(s) not in the initial library. For those element spaces that retain a stable proposed CTMH, we repeat the screening procedure described in ref 3 for the existing hydrides. We note that we continue to perform calculations for all proposed phases in a retained element space, regardless of whether or not the given materials were predicted to be stable initially. This is to ensure that proposed phases that are dynamically stabilized through vibrational effects can be identified for element spaces with a candidate proposed material.

If a given proposed material is not predicted to be stable for any given round of screening, this suggests that a CTMH with that composition will not be observed experimentally. Our calculations cannot preclude, however, the possibility that a CTMH will form in a lower energy crystal structure not studied here. While DFT-based crystal structure prediction methods exist,[18−22] in this work we take advantage of the prior knowledge that known CTMHs tend to form in a given set of prototype structures and maintain charge neutrality.

Computational Details. Computational details for this work are the same as those used in our previous screening of known compounds, but are included here for clarity.[3] Plane-wave DFT calculations were carried out via VASP[23−27] using the projector augmented wave (PAW) method with the PW91 GGA functional to describe exchange-correlation effects.[28−30] The recommended PAW pseudopotentials listed in the VASP manual were selected for each element.[31] Experimental crystal structures for known compounds were taken to be the low temperature, low pressure configurations of target compositions from the ICSD.[14,15] Pymatgen automation tools and Custodian error handling tools were utilized to manage the DFT setup and job management.[32,33]

The conjugate gradient method was used to relax volume, shape, and ion positions of compound primitive cells until forces on each atom were less than 0.03 eV Å^{-1} and electronic steps were converged to within 10^{-5} eV. Methfessel−Paxton smearing with a width of 0.2 eV was applied. On the basis of convergence testing described in ref [3], we found that a minimum density of 4000 *k*-points/(number of atoms per unit cell) distributed evenly along the reciprocal lattice and 400 eV cutoff energy vectors converges ΔE_0 to within 0.3 kJ mol^{-1} (3 meV atom^{-1}), and we adopt these settings for all solids in this study. Γ-centered grids were used for hexagonal symmetries for faster convergence. Monkhorst−Pack meshes were used for all other symmetries. The initial library of existing materials utilized a hierarchical scheme in the style of Jain et al.[33] and Curtarolo et al.[34] to determine whether or not the ferromagnetic spin polarity contribution to the ground state energy is significant or not.[3] Only materials with magnetic moments greater than 0.025 μ_B atom^{-1} were relaxed using spin-polarized calculations. No attempt was made to search for antiferromagnetic ground states for computational speed because most CTMHs are diamagnetic. We did not perform DFT calculations with spin-polarization for proposed materials. However, interesting element spaces could be studied more rigorously if the magnetic properties were desired.

For materials retained for round 2 screening, we performed phonon calculations using 2 × 2 × 2 supercells, except where indicated, with *k*-points adjusted to maintain the same grid density as used in the initial volume relaxations. Convergence calculations described in ref 3 found that supercell size is not expected to significantly affect the relative stabilities of materials in the studied element spaces. Rhombohedral supercells were used for hexagonal symmetries based on the guidelines of Parlinski.[35] The conjugate gradient method was used to first relax volume, shape, and ion positions until forces on each atom were less than 10^{-4} eV Å^{-1} and electronic steps were converged to within 10^{-7} eV. The VDOS was determined using the supercell approach using a default ion displacement of ±0.01 Å[36] within the simple harmonic approximation, which neglects anharmonic effects. The vibrational contribution to the Helmholtz free energy for the solid compounds, $F^{vib}(T)$, was computed using the VDOS with uniform *q*-point meshes to sample the Fourier components of the dynamical matrix that ensured F^{vib} (T = 2000 K) for each compound was converged to within 1 kJ mol^{-1}.

RESULTS

Initial Proposed CTMH Stability Calculations. We first relaxed crystal structures for the 149 proposed CTMHs displayed in Figure 2 using DFT at the moderate force and electronic energy convergence criteria. Relaxed geometrical parameters for these materials are listed in Table S.1 in the Supporting Information. We then computed initial GCLP phase diagrams (no F^{vib} for solid phases) for 102 element spaces, including the 71 element spaces not previously considered in our screening of known compounds[3] summarized in Figure 3, with >450 compound entries from the existing and proposed Round 1 materials libraries shown in Tables S.1 from the Supporting Information of ref 3 and Table S.1 in the Supporting Information of this work, respectively. If a proposed material from a new element space was predicted to have T_d/$T_{d,binary} \geq 1$, we added any additional simulation ready binary intermetallic compounds that could form in the element space from the ICSD to the GCLP input library.[14,15] Overall, 29 new binary intermetallic compounds listed in Table S.2 in the Supporting Information were incorporated into the materials library from the 24 new element spaces with stable proposed phases. As previously observed in ref 3, these intermetallics are concentrated among certain element combinations with 25 of

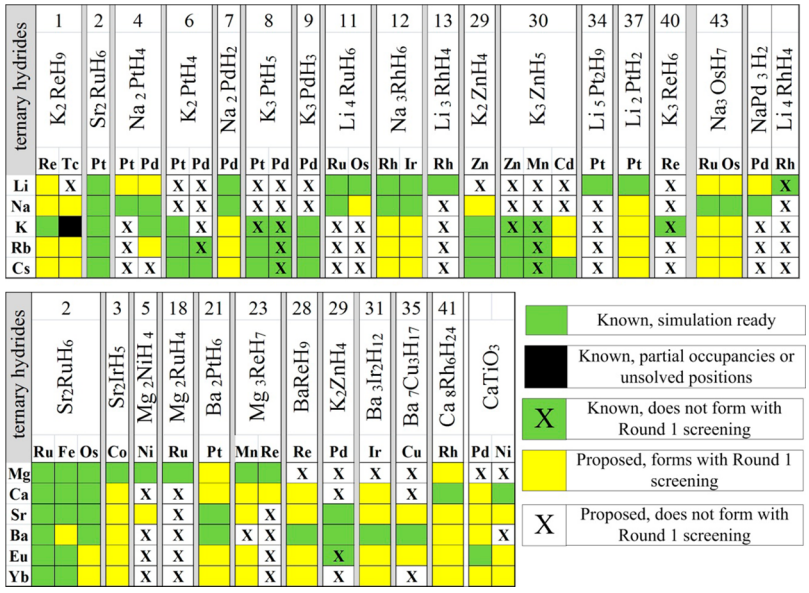

Figure 5. Initial stability prediction for 149 proposed and experimentally known ternary ($M-Tr-$H) CTMH materials based on Round 1 level DFT calculations (no vibrational corrections to free energy) and GCLP minimization. Known CTMHs are from the Yvon and Renaudin 2005 Review[1] and the ICSD. Calculations include additional intermetallic phases from the ICSD for new ternary element spaces that meet initial criterion $T_d/T_{d,binary} \geq 1$.

the 29 intermetallics completing the Ca−Pd, Eu−Pt, Eu−Rh, Mg−Rh, and Pd−Yb element spaces.

Figure 5 shows the initial prediction of stable ternary CTMHs based on the round 1 screening. If a proposed space was found to form at any T, P within the studied ranges, that is, $0 \leq T$ (K) ≤ 2000 and 10^{-6}, 10^{-4}, 10^{-2}, 1, and 100 bar H_2, it is shown in solid yellow. If a compound was not observed in the set of stable mixtures over the tested chemical potential ranges, it is shown with an "X". 76 of the 149 hypothetical materials are calculated to be thermodynamically viable based on these initial calculations. Decomposition pathways and T_d's for these are listed in Table S.1 in the Supporting Information. We reiterate that additional intermetallics for new element spaces were only included if the stable CTMH met the initial enhanced stability screening criterion. For example, the Eu−Pt and Yb−Pt element spaces each have several intermetallic phases, but only the intermetallics for Eu−Pt were included since the initial stability calculation indicated Eu_2PtH_6 had $T_d/T_{d,binary} = 1.01$ whereas Yb_2PtH_6 had $T_d/T_{d,binary} = 0.98$. After including the Eu−Pt intermetallics, the T_d for Eu_2PtH_6 drops from 1500 to 870 K since it is destabilized by Eu_5Pt_4. It is reasonable to assume that Yb_2PtH_6 with the element space's close relationship with the Eu−Pt−H system would similarly be further destabilized by an intermetallic phase.

Figure 5 shows that several prototypes have stable compounds that form for the entire series of tested cations with the same valence. For example, Li_2PdH_2 and Na_2PdH_2 compounds were known to crystallize experimentally in the 7−Na_2PdH_2 prototype structure. On the basis of our initial calculations, K^+, Rb^+, and Cs^+ materials may also be observed. With the exception of Li_2PdH_2, which decomposes to a mixture of LiPd, LiH, and H_2, the Na, K, Rb, and Cs compounds are predicted to be the most thermodynamically stable hydride phases in the respective element spaces, releasing H_2 to form the pure metals at high temperature based on round 1 calculations. Similarly, our calculations indicate that 12−Na_3RhH_6, 37−Li_2PtH_2, 43−Na_3OsH_7, 2−Sr_2RuH_6, 21−Ba_2PtH_6, and 41−$Ca_8Rh_6H_{24}$ prototypes have stable compounds that span the entire series of tested cations of the same valence. This is impressive since the ionic radii vary widely from approximately 0.9−1.81 Å for the alkali metals and 0.86−1.49 Å for the alkaline earth metals.[17]

The calculations above include only ground state energies of the condensed phases with T and P effects controlled through the hydrogen chemical potential. From our previous screening of existing materials,[3] we know that certain prototypes, in particular 8−K_3PtH_5 and 30−K_3ZnH_5, are dynamically stabilized through vibrational contributions. Materials that crystallize in these prototype structures might only be predicted to form if studied at the round 2 level of screening to account for these vibrational contributions. In some cases, the experimental structure is not predicted to form at this level of theory. For example, Rb_2PdH_4_p ("_p" indicates a proposed material) is calculated to be thermodynamically stable in the tetragonal 4−Na_2PtH_4 structure, but only the tetragonal 6−K_2PtH_4 crystal has been observed experimentally. As we discuss below, when this material is studied at the higher level of theory, the experimentally observed 6−K_2PtH_4 phase is recovered. A similar situation occurs for Li_4RhH_4. Figures S.1 and S.2 in the Supporting Information show the energies above the complex hull at 0 K for the unstable proposed CTMHs. Positive convex hull energies reflect endothermic formation energies for the given entry from the thermodynamically preferred combination of compounds.[37] Compounds with convex hull energies close to zero are in close competition energetically with the most stable states.

Round 1 Thermodynamic Screening. Table S.1 in the Supporting Information lists the calculated decomposition pathways for all stable proposed CTMH materials at the round 1 level of screening. Figure 6 shows the thermodynamic stabilities of these compounds based on the final screening criteria. Twenty-eight materials have estimated $T_d/T_{d,binary} \geq 1$ and 12 operate at high temperature, $T_d \geq 1000$ K. Of the materials with enhanced stability relative to the binary hydrides,

dx.doi.org/10.1021/ic501992x | Inorg. Chem. 2014, 53, 11849−11860

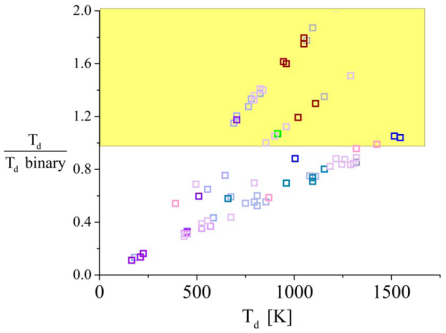

Figure 6. Relative and absolute thermal stabilities for stable proposed ternary CTMHs predicted with round 1 level of screening. Color indicates structure prototype. Materials in the shaded area meet the round 1 screening criterion for enhanced stability relative to the binary hydrides and are retained for round 2 screening.

8, 10, and 5 are Cs, Rb, and K-based materials, respectively. We add to these Sr_2NiH_4 with $T_d/T_{d,binary}$ = 0.85 and T_d = 1320 K since the T_d (SrH_2) is significantly overestimated based on the ground state calculation by 360 K and Ni is a common metal, which may be interesting for the NGNP and other high temperature industrial applications. These candidate materials are listed in Table 1, and the thermodynamic stabilities of the referenced binary hydrides computed at the same level of theory are available in Table S.3 in the Supporting Information.

This list comprises 28 element spaces, including 21 new element spaces for which a CTMH is not currently known to form experimentally based on current entries in the ICSD.[14,15] In most cases the most stable ternary hydride in the element space releases hydrogen and forms a mixture of the pure metal species. Na_2PtH_2_p is the only example of a ternary hydride with enhanced stability that is destabilized by an intermetallic phase.

Round 2 Thermodynamic Screening. We computed phase diagrams at the round 2 level of theory for the 28 element spaces retained from round 1 for $0 \leq T$ (K) ≤ 2000 at $P = 10^{-6}$, 10^{-4}, 10^{-2}, 1, and 100 bar H_2. In all, we computed the VDOS for 56 proposed CTMHs, including the 30 candidate materials listed in Table 1 and 27 other proposed CTMHs that complete the target element spaces, but that do not meet the initial screening criterion. The updated structural parameters for these materials are available in Table S.4 in the Supporting Information. In general we used 2 × 2 × 2 supercells to compute phonon properties of the materials in this study. However, for computational expediency, we performed phonon calculations using 1 × 1 × 1 unit cells for Cs_3RhH_4, Cs_3RhH_6, Cs_3RuH_7, K_3OsH_7, K_3IrH_6, K_3RhH_6, Cs_3IrH_6, Cs_3OsH_7, Rb_3IrH_6, Rb_3OsH_7, Rb_3RhH_4, Rb_3RhH_6, and Cs_2TcH_9. We also neglected the proposed materials Rb_4OsH_6 or Cs_4OsH_6 in the 11−Li_4RuH_6 prototype, which are not predicted to form within the range of studied chemical potentials on the basis of round 1 screening because of computational cost. K_4OsH_6 in

Table 1. Round 1 Candidates with Enhanced Thermodynamic Stability Relative to Binary Hydrides[a]

CTMH	structure prototype	T_d (K)	decomposition pathway	ΔE_0 (kJ mol^{-1} H_2)
Eu_2OsH_6_p	2−Sr_2RuH_6	1545	$^1/_3Eu_2OsH_6$_p ↔ $^2/_3Eu + {}^1/_3Os + H_2$	203.8
Yb_2OsH_6_p	2−Sr_2RuH_6	1515	$^1/_3Yb_2OsH_6$_p ↔ $^1/_3Os + {}^2/_3Yb + H_2$	200.2
Sr_2NiH_4_p	5−Mg_2NiH_4	1320	$^1/_2Sr_2NiH_4$_p ↔ $^1/_2Ni$ + Sr + H_2	165.3
K_2PtH_2_p	37−Li_2PtH_2	1290	K_2PtH_2_p ↔ Pt + 2K + H_2	160.4
Rb_2PtH_2_p	37−Li_2PtH_2	1215	Rb_2PtH_2_p ↔ Pt + 2Rb + H_2	147.5
Cs_2PtH_2_p	37−Li_2PtH_2	1215	Cs_2PtH_2_p ↔ $Cs_2Pt + H_2$	147.2
K_2PdH_2_p	7−Na_2PdH_2	1155	K_2PdH_2_p ↔ 2K + Pd + H_2	135.6
K_3IrH_6_p	12−Na_3RhH_6	1110	$^1/_3K_3IrH_6$_p ↔ K + $^1/_3Ir + H_2$	129.5
Cs_2PdH_2_p	7−Na_2PdH_2	1095	Cs_2PdH_2_p ↔ Pd + 2Cs + H_2	126.4
Rb_2PdH_2_p	7−Na_2PdH_2	1065	Rb_2PdH_2_p ↔ Pd + 2Rb + H_2	121.4
Rb_3IrH_6_p	12−Na_3RhH_6	1050	$^1/_3Rb_3IrH_6$_p ↔ $^1/_3Ir$ + Rb + H_2	119.6
Cs_3IrH_6_p	12−Na_3RhH_6	1050	$^1/_3Cs_3IrH_6$_p ↔ Cs + $^1/_3Ir + H_2$	117.4
K_3RhH_6_p	12−Na_3RhH_6	1020	$^1/_3K_3RhH_6$_p ↔ K + $^1/_3Rh + H_2$	113.8
Rb_3RhH_6_p	12−Na_3RhH_6	960	$^1/_3Rb_3RhH_6$_p ↔ Rb + $^1/_3Rh + H_2$	103.9
Na_2PtH_2_p	37−Li_2PtH_2	960	Na_2PtH_2_p ↔ $^3/_2Na + {}^1/_2NaPt_2 + H_2$	103.6
Cs_3RhH_6_p	12−Na_3RhH_6	945	$^1/_3Cs_3RhH_6$_p ↔ Cs + $^1/_3Rh + H_2$	101.7
Na_4OsH_6_p	11−Li_4RuH_6	915	$^4/_3Na_4OsH_6$_p ↔ $^4/_3Na + {}^1/_3Os + H_2$	95.5
K_3OsH_7_p	43−Na_3OsH_7	900	$^2/_7K_3OsH_7$_p ↔ $^2/_7Os + {}^6/_7K + H_2$	92.7
K_3RuH_7_p	43−Na_3OsH_7	855	$^2/_7K_3RuH_7$_p ↔ $^6/_7K + {}^2/_7Ru + H_2$	85.8
Rb_3OsH_7_p	43−Na_3OsH_7	840	$^2/_7Rb_3OsH_7$_p ↔ $^6/_7Rb + {}^2/_7Os + H_2$	84.3
Cs_3OsH_7_p	43−Na_3OsH_7	825	$^2/_7Cs_3OsH_7$_p ↔ $^2/_7Os + {}^6/_7Cs + H_2$	82.5
Rb_2PdH_4_p	4−Na_2PtH_4	825	Rb_2PdH_4_p ↔ Rb_2PdH_2_p + H_2	80.8
Rb_3RuH_7_p	43−Na_3OsH_7	795	$^2/_7Rb_3RuH_7$_p ↔ $^2/_7Ru + {}^6/_7Rb + H_2$	77.5
Cs_3RuH_7_p	43−Na_3OsH_7	795	$^2/_7Cs_3RuH_7$_p ↔ $^6/_7Cs + {}^2/_7Ru + H_2$	75.8
Cs_2ReH_9_p	1−K_2ReH_9	780	$^2/_9Cs_2ReH_9$_p ↔ $^4/_9Cs + {}^2/_9Re + H_2$	73.3
Rb_2ReH_9_p	1−K_2ReH_9	765	$^2/_9Rb_2ReH_9$_p ↔ $^2/_9Re + {}^4/_9Rb + H_2$	72.1
Cs_2TcH_9_p	1−K_2ReH_9	705	$^2/_9Cs_2TcH_9$_p ↔ $^2/_9Tc + {}^4/_9Cs + H_2$	62.2
Rb_3CdH_5_p	30−K_3ZnH_5	705	$^2/_5Rb_3CdH_5$_p ↔ $^6/_5Rb + {}^2/_5Cd + H_2$	61.9
Rb_2TcH_9_p	1−K_2ReH_9	690	$^2/_9Rb_2TcH_9$_p ↔ $^2/_9Tc + {}^4/_9Rb + H_2$	61.0

[a]"_p" indicates a proposed material.

dx.doi.org/10.1021/ic501992x | Inorg. Chem. 2014, 53, 11849−11860

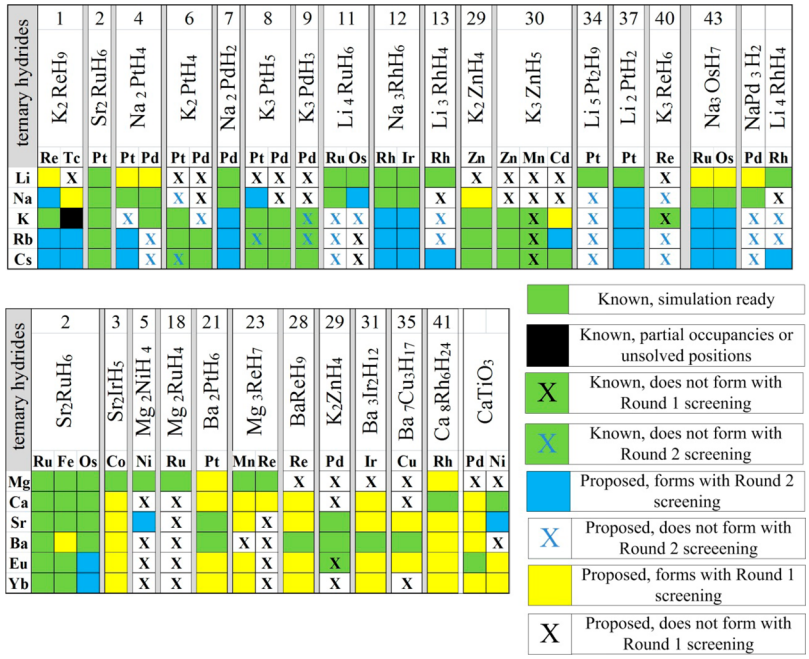

Figure 7. Final stability prediction for 149 proposed and experimentally known ternary ($M-Tr-$H) CTMH materials based on round 1 and round 2 levels of theory. Known CTMHs are from the Yvon and Renaudin 2005 Review[1] and the ICSD. Stable materials form between $0 \leq T$ (K) ≤ 2000 for $P = 10^{-6}$, 10^{-4}, 10^{-2}, 1, and 100 bar H_2. Calculations include additional intermetallic phases from the ICSD for new ternary element spaces that meet initial criterion $T_d/T_{d,binary} \geq 1$.

the same prototype was not calculated to form at either round 1 or round 2 level of theory. K_4RuH_6, Cs_4RuH_6, and Rb_4RuH_6 in the 11−Li_4RuH_6 prototype were studied with round 2 level calculations, and none were predicted to be stable within the studied T, P range. For these reasons, neglecting Rb_4OsH_6 and Cs_4OsH_6 is not expected to affect the final phase stability results.

Figure 7 displays the mapping of the final stability predictions for both round 1 calculations (stable = solid yellow and unstable = black "X") based on ground state energies for the condensed phases and round 2 level calculations (stable = solid blue and unstable = blue "X") that include vibrational contributions to the free energies in the prediction of phase diagrams with the GCLP method. If a material was identified as a stable component for the hydrogen chemical potentials associated with the T and P range studied, it is labeled as "forming". On the basis of our calculations, 34 and 46 proposed hydrides of the initial 149 hypothetical materials are predicted to be thermodynamically stable based on round 2 and round 1 levels of theory, respectively. All of the materials predicted to be stable based on round 1 calculations that were studied at the higher level of theory were also predicted to be thermodynamically stable when accounting for vibrational effects.

Figure 7 indicates there are many hypothetical materials that should be thermodynamically preferred states in the given element spaces. These calculations assume that compound formation is thermodynamically controlled, with no consideration of kinetics. Practically, kinetic limitations can be problematic with solid state reactions. CTMH synthesis is typically performed at high hydrogen pressures and temperatures (~500−800 K), and it can be difficult to obtain single crystals for high resolution materials characterization.[1,38] Bronger and Auffermann note that for transition metals in multiple oxidation states across ternary hydrides, a higher reaction pressure is required to achieve the higher oxidation state.[38] Higher oxidation states have been particularly difficult to achieve experimentally when light cations like Li or Na are employed.[38] New synthesis techniques may be required to overcome kinetic barriers to reach the thermodynamically preferred mixture of compounds. This area deserves future study.

Figure 8 displays the round 2 absolute and relative decomposition temperatures for stable proposed CTMHs at

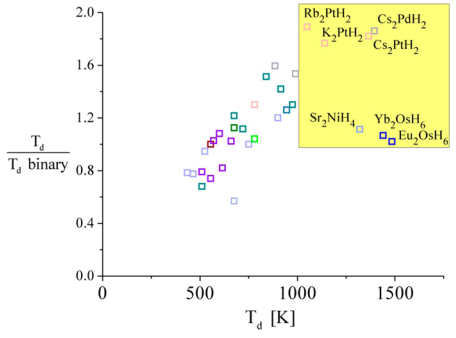

Figure 8. Relative and absolute thermal stabilities for stable proposed ternary CTMHs predicted with round 2 level of screening. Color indicates structure prototype. Materials in the shaded area are the final candidates that meet the round 2 screening criteria for both enhanced stability relative to the binary hydrides and $T_d > 1000$ K.

1 bar H_2. Relevant decomposition reactions and thermodynamic properties for all of the proposed materials that form for $P = 1$ bar H_2 are listed in Table 2. Seven of the proposed materials meet both screening criteria, that is, $T_d/T_{d,binary} \geq 1$ and $T_d \geq 1000$ K. By comparison, 13 of the known CTMHs have enhanced stability relative to the binary hydrides and also release hydrogen at high temperature.[3] As with the top candidates identified from the known materials, two of the

dx.doi.org/10.1021/ic501992x | Inorg. Chem. 2014, 53, 11849−11860

Table 2. Thermodynamic Properties of Stable Proposed Phases at P = 1 bar H_2 from Round 2 Calculations, Including Vibrational Corrections to the Helmholtz Free Energy for Condensed Phases[a]

CTMH	T_d	decomposition pathway	$\Delta H°$	$\Delta S°$	$\Delta H(T_d)$
		final candidates			
Eu_2OsH_6_p	1485	$^1/_3Eu_2OsH_6$_p ↔ $^2/_3Eu + ^1/_3Os + H_2$	197.6	0.131	191.0
Yb_2OsH_6_p	1440	$^1/_3Yb_2OsH_6$_p ↔ $^1/_3Os + ^2/_3Yb$_ + H_2	193.4	0.132	187.6
Cs_2PdH_2_p	1395	Cs_2PdH_2_p ↔ Pd + 2Cs + H_2	124.8	0.101	101.3
Cs_2PtH_2_p	1365	Cs_2PtH_2_p ↔ $Cs_2Pt + H_2$	144.3	0.111	130.3
Sr_2NiH_4_p	1320	$^1/_2Sr_2NiH4$_p ↔ $^1/_2Ni$ + Sr + H_2	166.6	0.128	158.4
K_2PtH_2_p	1140	K_2PtH_2_p ↔ 2K + Pt + H_2	159.5	0.140	154.8
Rb_2PtH_2_p	1050	Rb_2PtH_2_p ↔ Pt + 2Rb + H_2	147.0	0.141	143.3
		screened candidates			
K_2PdH_2_p	990	K_2PdH_2_p ↔ 2K + Pd + H_2	137.2	0.140	133.2
Cs_3IrH_6_p	975	$^1/_3Cs_3IrH_6$_p ↔ Cs + $^1/_3Ir + H_2$	113.1	0.119	106.8
Cs_2PtH_4_p	945	Cs_2PtH_4_p ↔ Cs_2PtH_2_p + H_2	121.3	0.126	121.2
K_3IrH_6_p	915	$^1/_3K_3IrH_6$_p ↔ K + $^1/_3Ir + H_2$	125.9	0.137	125.1
Cs_2ReH_9_p	900	$^2/_9Cs_2ReH_9$_p ↔ $^2/_9Re + ^4/_9Cs + H_2$	81.9	0.085	91.9
Rb_2PdH_2_p	885	Rb_2PdH_2_p ↔ Pd + 2Rb + H_2	123.4	0.140	120.6
Rb_3IrH_6_p	840	$^1/_3Rb_3IrH_6$_p ↔ $^1/_3Ir$ + Rb + H_2	116.5	0.138	116.1
Cs_3RhH_4_p	780	$^1/_2Cs_3RhH_4$_p ↔ $^3/_2Cs + ^1/_2Rh + H_2$	88.1	0.116	101.5
Na_2PtH_2_p	780	Na_2PtH_2_p ↔ $^3/_2Na + ^1/_2NaPt_2 + H_2$	101.8	0.131	82.6
Cs_2TcH_9_p	750	$^2/_7Cs_2TcH_9$_p ↔ $^2/_7Tc + ^4/_7CsH + H_2$	80.9	0.116	69.5
K_3RhH_6_p	720	$^1/_3K_3RhH_6$_p ↔ $^1/_3Rh$ + K + H_2	114.1	0.156	118.4
Na_4OsH_6_p	675	$^1/_3Na_4OsH_6$_p ↔ $^1/_3Os + ^4/_3Na + H_2$	92.5	0.137	106.9
Rb_3RhH_6_p	675	$^1/_3Rb_3RhH_6$_p ↔ $^1/_3Rh$ + Rb + H_2	104.4	0.153	93.5
$SrNiH_3$_p	675	2$SrNiH_3$_p ↔ Ni + Sr_2NiH4_p + H_2	94.6	0.141	94.5
K_3OsH_7_p	660	$^2/_7K_3OsH_7$_p ↔ $^2/_7Os + ^6/_7K + H_2$	87.7	0.133	88.9
Cs_3OsH_7_p	615	$^1/_2Cs_3OsH_7$_p ↔ $^3/_2CsH + ^1/_2Os + H_2$	74.1	0.117	78.4
Rb_3OsH_7_p	600	$^2/_7Rb_3OsH_7$_p ↔ $^6/_7Rb + ^2/_7Os + H_2$	80.0	0.134	81.1
Rb_3RuH_7_p	570	$^2/_7Rb_3RuH_7$_p ↔ $^2/_7Ru + ^6/_7Rb + H_2$	75.7	0.134	76.7
Cs_3RuH_7_p	555	$^1/_2Cs_3RuH_7$_p ↔ $^1/_2Ru + ^3/_2CsH + H_2$	66.5	0.119	46.5
Rb_3CdH_5_p	555	Rb_3CdH_5_p ↔ Cd + 3RbH + H_2	45.6	0.110	69.9
Rb_2ReH_9_p	525	$^2/_7Rb_2ReH_9$_p ↔ $^2/_7Re + ^4/_7RbH + H_2$	74.8	0.138	82.6
Cs_3RhH_6_p	510	Cs_3RhH_6_p ↔ Cs_3RhH_4_p + H_2	119.4	0.232	81.9
K_3RuH_7_p	510	$^1/_2K_3RuH_7$_p ↔ $^1/_2Ru + ^3/_2KH + H_2$	76.0	0.146	130.4
Rb_2TcH_9_p	435	$^2/_7Rb_2TcH_9$_p ↔ $^2/_7Tc + ^4/_7RbH + H_2$	60.2	0.136	64.9

[a]Standard conditions (300 K, 1 bar H_2). T_d (K), ΔH (kJ mol^{-1} H_2), ΔS (kJ K^{-1} mol^{-1} H_2).

top proposed materials are predicted to crystallize in the 2−Sr_2RuH_6 cubic prototype. Interestingly, where only its namesake was known to crystallize in the 37−Li_2PtH_2 prototype, our calculations predict that K_2PtH_2_p, Rb_2PtH_2_p, and Cs_2PtH_2_p are thermodynamically preferred at high temperature. Cs_2PdH_2 and Sr_2NiH_4, in the 7−Na_2PdH_2 and 5−Mg_2NiH_4 structures, respectively, are also the only materials studied, either existing or proposed, that meet the screening criteria and crystallize with those symmetries.

Phase Diagrams for Final Candidates. *Eu_2OsH_6_p and Yb_2OsH_6_p (2−Sr_2RuH_6 Prototype).* Eu_2RuH_6,[39] Eu_2FeH_6,[40] Yb_2RuH_6,[41,42] and Yb_2FeH_6[1] have been synthesized in the fcc 2−Sr_2RuH_6 prototype (Na_2PtCl_6-type structure). Round 1 (ground state) calculations for Eu(Yb)−Fe−H and round 2 (phonon-corrected) calculations for Eu(Yb)−Ru−H from our previous calculations[3] verify that these phases are thermodynamically preferred. Our calculations in this work indicate that Eu_2OsH_6_p and Yb_2OsH_6_p in this prototype are also thermodynamically stable phases. The calculated phase diagrams for 1 bar H_2 are displayed in Figure 9. In both cases, the only known competing compounds are the pure metals and binary hydrides. While Huang et al. attempted syntheses for some metal combinations (Ca−Fe, Sr−Fe, Eu−Fe, Mg−Ru, Mg−Os, and Ca−Os), resulting in the characterizations of known 2−Sr_2RuH_6 materials shown in Figure 7, they do not report attempting to form ternary hydrides from the combination of Eu−Os−H.[40] To our knowledge, no experimental investigations of these ternary hydrides have been carried out.

Cs_2PdH_2_p (7−Na_2PdH_2 Prototype). Stable compounds have been synthesized and characterized for Li_2PdH_2[43] and Na_2PdH_2[43−45] in the tetragonal $I4/mmm$ 7−Na_2PdH_2 crystal structure with linear H−Pd−H complexes. However, no experimentally identified CTMH has been reported for Cs_2PdH_2_p in this prototype structure. Synthesis of Cs_2PdH_4 has been carried out by Bronger and Auffermann, and they found that the high temperature form of the ternary hydride for the M/Pd ratio of 2:1 is a cubic K_2PtCl_6-type structure with a hydrogen partial occupancy factor of 2/3.[46] Materials with partial occupancies are not considered in the current work. However, comparing the ordered compounds without partial occupancies, we have computed the phase diagrams for the Cs−Pd−H system both based only on known compounds and with the proposed phases, shown in Figure 10. We predict a stable high temperature Cs_2PdH_2_p compound crystallizes in the 7−Na_2PdH_2 prototype. The highest temperature achieved

dx.doi.org/10.1021/ic501992x | Inorg. Chem. 2014, 53, 11849−11860

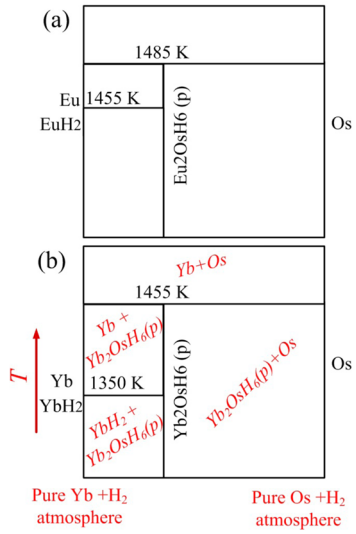

Figure 9. Predicted phase diagrams based on GCLP minimization including vibrational free energies for (a) Eu−Os−H and (b) Yb−Os−H at P = 1 bar H_2 (not drawn to scale). The horizontal axis shows molar ratio of metals at a given composition. The pure cation and pure transition metals are the far left and right axes, respectively. Temperature increases along the vertical axis. As shown for the Yb−Os−H system, each box represents a unique mixture of stable compounds. For a given T, this stable mix (obtained from the GCLP method) can be read by drawing a horizontal line at that T through the intersecting vertical lines, which represent the stable stoichiometric compounds.

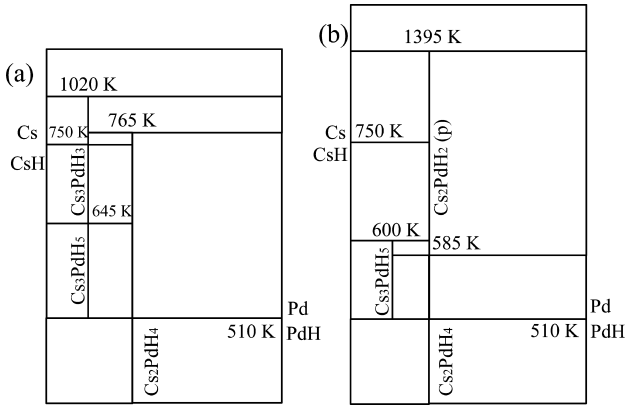

Figure 10. Predicted phase diagrams based on GCLP minimization including vibrational free energies for the Cs−Pd−H at P = 1 bar H_2 with (a) only known materials and (b) proposed phases.

for a hydride phase based on known materials is T_d = 1020 K for Cs_3PdH_3. Including the proposed phase increases this predicted stability to T_d = 1395 K for Cs_2PdH_2_p. The Cs_3PdH_3 phase is destabilized by the proposed phase. If a Cs_2PdH_4 material with partial hydrogen occupancies is thermodynamically stable, but not included in these calculations, it would have a lower free energy than the Cs_2PdH_2_p phase and destabilize the Cs_3PdH_x hydrides to a greater degree. If a more stable ternary hydride exists in this elemental system, our calculations can be considered a lower limit to the hydrogen release temperature for Cs−Pd hydrides.

K_2PtH_2_p, Rb_2PtH_2_p, Cs_2PtH_2_p (37−Li_2PtH_2 Prototype). The 37−Li_2PtH_2 structure prototype is an orthorhombic distortion of tetragonal Li_2PdH_2 (7−Na_2PdH_2 prototype) with linear $[PtH_2]^{2-}$ complexes.[1] 37−Li_2PtH_2 has been synthesized experimentally by decomposing $Li_5Pt_2H_9$ at 493 K in an argon atmosphere into $2Li_2PtH_2 + LiH + 2H_2$.[47,48] Our calculations for the Li−Pt−H system based on round 1 level ground state energies for condensed phases, including all known binary intermetallic phases, are consistent with the experiment. We predict $Li_5Pt_2H_9$ decomposes at 615 K with P = 1 bar H_2 via

$$\frac{1}{2}Li_5Pt_2H_9 \leftrightarrow Li_2PtH_2 + \frac{1}{2}LiH + H_2 \quad (1)$$

and that Li_2PtH_2 releases hydrogen at 840 K via

$$Li_2PtH_2 \leftrightarrow Li_2Pt + H_2 \quad (2)$$

It appears that no attempt has been made to synthesize K_2PtH_2_p, Rb_2PtH_2_p, or Cs_2PtH_2_p experimentally, but our calculations indicate that these compositions are stable at high temperature in the 37−Li_2PtH_2 prototype crystal structure. Unlike the Li−Pt−H element space, no other alkali metal-substituted hydride is stable in the 34−$Li_5Pt_2H_9$ prototype, and hydrides that form from a 2 M: 1 Pt ratio in the K−Pt−H and Rb−Pt−H systems are predicted to decompose via (eqs 3−5) with T_d (M = K, M = Rb) shown in parentheses:

$$M_2PtH_6 \leftrightarrow M_2PtH_4 + H_2 \ (555, 570\ K) \quad (3)$$

$$M_2PtH_4 \leftrightarrow M_2PtH_2\_p + H_2 \ (660, 975\ K) \quad (4)$$

$$M_2PtH_2\_p \leftrightarrow 2M + Pt + H_2 \ (1140, 1050\ K) \quad (5)$$

The binary intermetallic Cs_2Pt, the analog of which is not known for the K−Pt or Rb−Pt systems, destabilizes Cs_2PtH_2_p, and the hydrides at a 2 Cs/1 Pt ratio in the Cs−Pt−H system decompose via

$$Cs_2PtH_6 \leftrightarrow Cs_2PtH_4\_p + H_2 \ (T_d = 510\ K) \quad (6)$$

$$Cs_2PtH_4\_p \leftrightarrow Cs_2PtH_2\_p + H_2 \ (T_d = 945\ K) \quad (7)$$

$$Cs_2PtH_2\_p \leftrightarrow Cs_2Pt + H_2 \ (T_d = 1365\ K) \quad (8)$$

Besides the binary intermetallic that forms in the Cs−Pt space, the ternary CTMH Cs_2PtH_4_p is also predicted to form. On the basis of the calculated phase diagram at 100 bar H_2, we also note that Rb_2PtH_4_p (4−Na_2PtH_4) with $I4/mmm$ symmetry is stabilized over the known Rb_2PtH_4 (6−K_2PtH_4) with $P42/mmm$ symmetry. The main difference between these crystal structures is the rotation of the $[PtH_4]^{2-}$ square planar complex perpendicular to the tetragonal base for the $P42/mmm$ structure. Both materials have cubic or nearly cubic cation submatrices.[1] Our calculations do not account for disordered structures or structures with partial hydrogen occupancies. Experimentally, it has been observed that K_2PtH_4, Rb_2PtH_4, and Cs_2PtH_4 transition to disordered cubic structures similar to 2−Sr_2RuH_6 with 2/3 partial hydrogen occupancies close to room temperature.[1,38] If this disordered modification is a thermodynamically stable state, it is expected to have a lower free energy than the materials considered here, and hydrogen would be further stabilized in the structure. Our calculations can then be taken as a lower bound on the thermodynamic stability of CTMHs in the element spaces, again assuming that no high temperature binary intermetallic phase exists that is unknown at this time.

Calculated phase diagrams at P = 1 bar H_2 with and without proposed phases are shown in Figures 11−13 for K−Pt−H, Rb−Pt−H, and Cs−Pt−H, respectively. We highlight the

dx.doi.org/10.1021/ic501992x | Inorg. Chem. 2014, 53, 11849−11860

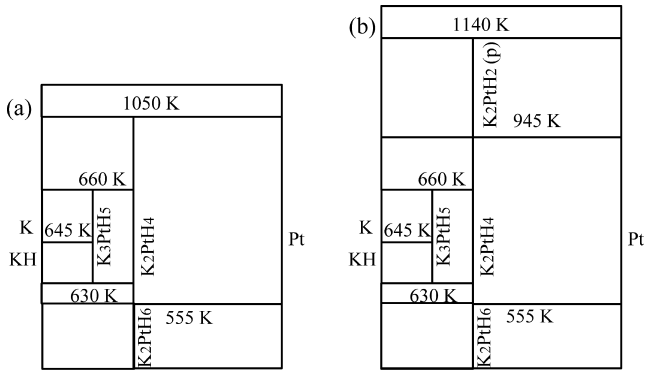

Figure 11. Predicted phase diagrams based on GCLP minimization including vibrational free energies for the K−Pt−H at P = 1 bar H_2 with (a) only known materials and (b) proposed phases.

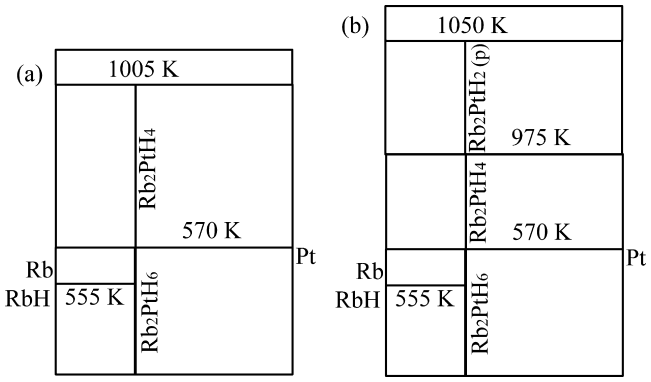

Figure 12. Predicted phase diagrams based on GCLP minimization including vibrational free energies for the Rb−Pt−H at P = 1 bar H_2 with (a) only known materials and (b) proposed phases.

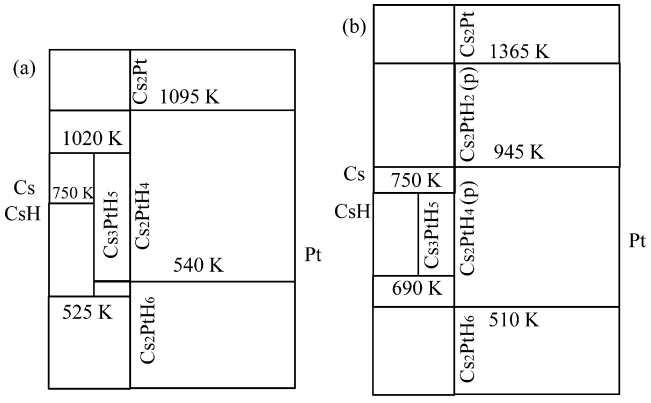

Figure 13. Predicted phase diagrams based on GCLP minimization including vibrational free energies for the Cs−Pt−H at P = 1 bar H_2 with (a) only known materials and (b) proposed phases.

increase in hydrogen release temperature when including the proposed phases for these element spaces. Experimentally, K_3PtH_5 decomposes at 673 K into KH and K_2PtH_4.[1] Our calculations predict a slightly less thermodynamically stable binary hydride, but cannot resolve the energy difference associated with 15 K or ∼2 kJ mol^{-1} H_2 (assuming $\Delta T_d \approx \Delta H/\Delta S$ and ΔS = 0.131 kJ K^{-1} mol^{-1} H_2). We can expect that the DFT resolves the relative stabilities of K_3PtH_5 and K_2PtH_4 with higher fidelity due to the broad difference in the predicted T_d of nearly 300 K. Our calculations do not capture the experimentally observed Rb_3PtH_5 phase for any of the studied hydrogen pressures. Since this composition is predicted to form in the similar Cs−Pt−H element space, this suggests that the DFT calculations are in error for this composition. For the Rb−Pt−H and Cs−Pt−H element spaces, the M_3PtH_5 composition is known to transition to a high temperature disordered cubic phase at 465 and 615 K, respectively. Again, our calculations do not consider disordered phases.

Sr_2NiH_4_p (5−Mg_2NiH_4 Prototype). On the basis of round 2 level calculations, Sr_2NiH_4_p is thermodynamically stable in the 5−Mg_2NiH_4 prototype structure. There are currently no known CTMHs that form in the Sr−Ni−H element space, which makes this and the other predicted stable proposed compound, $SrNiH_3$_p, unique among the materials studied in this paper. Figure 14 shows the predicted phase diagrams for

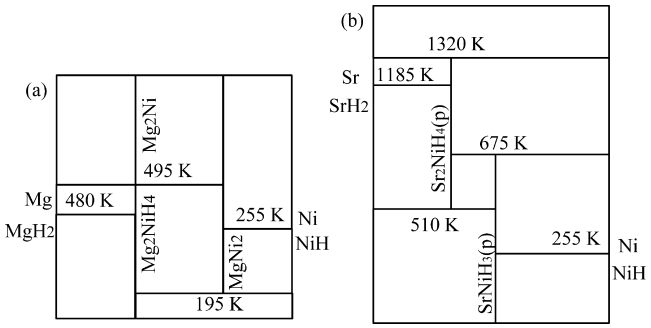

Figure 14. Predicted phase diagram based on GCLP minimization including vibrational free energies for (a) the known Mg−Ni−H and (b) proposed Sr−Ni−H element spaces at P = 1 bar H_2.

the known Mg−Ni−H and proposed Sr−Ni−H element spaces, including vibrational corrections, at P = 1 bar H_2. Literature reports for T_d of Mg_2NiH_4, which forms the intermetallic Mg_2Ni and hydrogen upon heating experimentally, are about 520 K.[49,50] However, other authors have reported values up to 673 K depending on the measurement method used.[49,51] Our calculations give T_d = 495 K for Mg_2NiH_4, in reasonable agreement with the experimental value. We neglected the high temperature disordered phase of Mg_2NiH_4, similar to 2−Sr_2RuH_6 with partial occupancies, and so our calculations may be taken as a lower limit on the thermal stability of this composition.[1]

To our knowledge, no attempt has been made to synthesize either Sr_2NiH_4_p or $SrNiH_3$_p. While there is a Sr_2Ni_3 intermetallic compound with partial occupancies, there is no known Sr_2Ni intermetallic compound that is analogous to the Mg_2Ni phase, and our calculations show that the hypothetical Sr_2NiH_4 decomposes to the elements and hydrogen at T_d = 1320 K. This represents the only compound, either from our previous screening of known CTMHs[3] or from the current work including similar hypothetical materials, that meets both screening criteria and that contains the relatively common Ni metal.

van't Hoff Plots. Figure S.3 in the Supporting Information shows the van't Hoff plots for the final candidate proposed materials from Table 2. Eu_2OsH_6_p and Yb_2OsH_6_p are the most stable of the hypothetical hydrides over the studied temperature range. The calculations predict that, at the highest temperatures, Cs_2PdH_2_p and Cs_2PtH_2_p are nearly as thermodynamically stable as the rare earth osmium hydrides.

dx.doi.org/10.1021/ic501992x | Inorg. Chem. 2014, 53, 11849−11860

This is primarily attributed to the low calculated entropy of reaction for the Cs-based materials.

Figure S.4 in the Supporting Information shows the van't Hoff plots for the most thermodynamically stable proposed and known CTMHs along with the associated binary hydrides. Several of the curves are nearly degenerate: (1, 3) Eu_2RuH_6 and Eu_2OsH_6_p, (2, 7) Yb_2OsH_6_p, EuH_2, and Yb_2RuH_6, (8, 5) YbH_2 and Ca_2RuH_6, and (6) CaH_2, where the number identifies the ordering of the material in the plot legend. In each case, the CTMH exhibits lower H_2 overpressures than the associated binary hydride, as expected. This work also shows that hypothetical hydrides of Eu and Yb are at least as thermodynamically stable as the most stable known CTMH. These curves represent the CTMHs with lowest overall hydrogen equilibrium pressures for the NGNP and other high temperature metal hydride applications and should be useful for determining operating parameters for such systems.

CONCLUSIONS

We have successfully used DFT and GCLP minimization calculations to screen a set of 149 proposed CTMH materials based on the prototype structures of known materials. Using a tiered approach for computational efficiency that computes the stable mixture of compounds pulled from a materials library for a given chemical potential, we predict that 81 of the 149 materials are thermodynamically preferred in the studied T, P range. Thirty-four were stable at the round 2 level of theory that accounts for vibrational effects, and 46 stable materials were indicated at only the round 1 level of theory based on ground state energies alone for condensed phases. Of these stable materials, seven meet the screening criteria of enhanced stability relative to the binary hydrides and high hydrogen release temperature for the NGNP and other high temperature metal hydride applications. Two of the proposed materials have hydrogen equilibrium pressures nearly identical to the most thermodynamically stable known materials. The calculated phase diagrams should be useful for setting operating limits for the hydrides. Of the materials we examined, Sr_2NiH_4 appears particularly appealing for the NGNP application because of its predicted stability and relatively low cost. Future computational work could focus on further characterizing the properties of the stable proposed materials, in particular electronic and magnetic properties that may be unique for the hypothetical materials.

ASSOCIATED CONTENT

Supporting Information

Listings are available of the studied materials lattice parameters and decomposition pathways, computed at the round 1 and round 2 levels of theory, convex hulls for unstable entries, and van't Hoff plots. This material is available free of charge via the Internet at http://pubs.acs.org.

AUTHOR INFORMATION

Corresponding Author

*E-mail: david.sholl@chbe.gatech.edu.

Notes

The authors declare no competing financial interest.

ACKNOWLEDGMENTS

This research was performed using funding received from the DOE Office of Nuclear Energy's Nuclear Energy University Programs.

REFERENCES

(1) Yvon, K.; Renaudin, G. Hydrides: Solid State Transition Metal Complexes. In *Encyclopedia of Inorganic Chemistry*, 2nd ed.; King, B. R., Ed.; John Wiley & Sons: Chichester, U.K., 2005; Vol. *III*, pp 1814−1846.
(2) Richardson, T. J.; Slack, J. L.; Armitage, R. D.; Kostecki, R.; Farangis, B.; Rubin, M. D. *Appl. Phys. Lett.* **2001**, *78*, 3047−3049.
(3) Nicholson, K. M.; Sholl, D. S. *Inorg. Chem.* **2014**, DOI: 10.1021/ic501990p.
(4) Bogdanović, B.; Reiser, A.; Schlichte, K.; Spliethoff, B.; Tesche, B. *J. Alloys Compd.* **2002**, *345*, 77−89.
(5) Felderhoff, M.; Bogdanović, B. *Int. J. Mol. Sci.* **2009**, *10*, 325−344.
(6) Gil, A.; Medrano, M.; Martorell, I.; Lázaro, A.; Dolado, P.; Zalba, B.; Cabeza, L. F. *Renewable Sustainable Energy Rev.* **2010**, *14*, 31−55.
(7) Harries, D. N.; Paskevicius, M.; Sheppard, D. A.; Price, T. E. C.; Buckley, C. E. *Proc. IEEE* **2012**, *100*, 539−549.
(8) U.S. DOE Nuclear Energy Research Advisory Committee and Generation IV International Forum. *A Technology Roadmap for Generation IV Nuclear Energy Systems*. Report Number 03-GA50034; U.S. DOE: Washington, DC, 2002.
(9) U.S. DOE Office of Nuclear Energy. *Next Generation Nuclear Plant Report to Congress*; U.S. DOE: Washington, DC, 2010.
(10) U.S. DOE. *The U.S. Generation-IV Implementation Strategy*. DOE Office of Nuclear Energy: Washington, DC, 2003.
(11) Sherman, S. R.; Adams, T. M. *Tritium Barrier Materials and Separation Systems for the NGNP*; U.S. DOE, Savannah River National Laboratory: Aiken, SC, 2008.
(12) NGNP Project. *Next Generation Nuclear Plant Project: Preliminary Project Plan*; Idaho National Laboratory: Idaho Falls, ID, 2007.
(13) Parker, S. F. *Coord. Chem. Rev.* **2010**, *254*, 215−234.
(14) FIZ Karlsruhe. *The Inorganic Crystal Structure Database (ICSD)*. http://www.fiz-karlsruhe.de/icsd.html.
(15) Bergerhoff, G.; Brown, I. D. In *Crystallographic Databases*; Allen, F. H., Bergerhoff, G., Severs, R., Eds.; International Union of Crystallography: Chester, U.K., 1987.
(16) Puhakainen, K.; Stoyanov, E.; Evans, M. J.; Leinenweber, K.; Haussermann, U. *J. Solid State Chem.* **2010**, *183*, 1785−1789.
(17) Shannon, R. *Acta Crystallogr.* **1976**, *32*, 751−767.
(18) Ke, X.; Kuwabara, A.; Tanaka, I. *Phys. Rev. B* **2005**, *71*, No. 184107.
(19) Wolverton, C.; Donald, J. S.; Akbarzadeh, A. R.; Ozoliņš, V. *J. Phys.: Condens. Matter* **2008**, *20*, No. 064228.
(20) Ozolins, V.; Akbarzadeh, A. R.; Gunaydin, H.; Michel, K.; Wolverton, C.; Majzoub, E. H. *J. Phys. Conf. Ser.* **2009**, *180*, No. 012076.
(21) Ozolins, V.; Majzoub, E. H.; Wolverton, C. *Phys. Rev. Lett.* **2008**, *100*, No. 135501.
(22) Majzoub, E. H.; Ozoliņš, V. *Phys. Rev. B* **2008**, *77*, No. 104115.
(23) Kresse, G.; Hafner, J. *Phys. Rev. B* **1993**, *47*, 558−561.
(24) Kresse, G.; Hafner, J. *Phys. Rev. B* **1994**, *49*, 14251−14269.
(25) Kresse, G.; Furthmüller, J. *Phys. Rev. B* **1996**, *54*, 11169−11186.
(26) Kresse, G.; Furthmüller, J. *Comput. Mater. Sci.* **1996**, *6*, 15−50.
(27) Sholl, D. S.; Steckel, J. A. *Density Functional Theory: A Practical Introduction*; John Wiley & Sons: Hoboken, NJ, 2009.
(28) Blöchl, P. E. *Phys. Rev. B* **1994**, *50*, 17953−17979.
(29) Kresse, G.; Joubert, D. *Phys. Rev. B* **1999**, *59*, 1758−1775.
(30) Perdew, J. P.; Chevary, J. A.; Vosko, S. H.; Jackson, K. A.; Pederson, M. R.; Singh, D. J.; Fiolhais, C. *Phys. Rev. B* **1992**, *46*, 6671−6687.
(31) Kresse, G.; Marsman, M.; Furthmüller, J. *Vienna Ab-Initio Simulation Package: VASP the Guide*; Computational Materials Physics: Vienna, 2014.
(32) Ong, S. P.; Richards, W. D.; Jain, A.; Hautier, G.; Kocher, M.; Cholia, S.; Gunter, D.; Chevrier, V. L.; Persson, K. A.; Ceder, G. *Comput. Mater. Sci.* **2013**, *68*, 314−319.
(33) Jain, A.; Hautier, G.; Moore, C. J.; Ping Ong, S.; Fischer, C. C.; Mueller, T.; Persson, K. A.; Ceder, G. *Comput. Mater. Sci.* **2011**, *50*, 2295−2310.

(34) Curtarolo, S.; Setyawan, W.; Hart, G. L. W.; Jahnatek, M.; Chepulskii, R. V.; Taylor, R. H.; Wang, S.; Xue, J.; Yang, K.; Levy, O.; et al. *Comput. Mater. Sci.* **2012**, *58*, 218−226.
(35) Parlinski, K. *PHONON*; Computing for Materials: Krakow, 2005.
(36) Togo, A.; Oba, F.; Tanaka, I. *Phys. Rev. B* **2008**, *78*, No. 134106.
(37) Wolverton, C.; Ozoliņš, V. *Phys. Rev. B* **2007**, *75*, No. 064101.
(38) Bronger, W.; Auffermann, G. *Chem. Mater.* **1998**, *10*, 2723−2732.
(39) Thompson, J. S.; Moyer, R. O.; Lindsay, R. *Inorg. Chem.* **1975**, *14*, 1866−1869.
(40) Huang, B.; Bonhomme, F.; Selvam, P.; Yvon, K.; Fischer, P. *J. Less-Common Met* **1991**, *171*, 301−311.
(41) Lindsay, R.; Moyer, R. O.; Thompson, J. S.; Kuhn, D. *Inorg. Chem.* **1976**, *15*, 3050−3053.
(42) Moyer, R. O., Jr; Gilson, D. F. R.; Toby, B. H. *J. Solid State Chem.* **2011**, *184*, 1895−1898.
(43) Kasowski, R. V.; Noreus, D.; Wang, L.; Whangbo, M. H. *Inorg. Chem.* **1992**, *31*, 4737−4739.
(44) Noréus, D.; Tomkinson, J. *Chem. Phys. Lett.* **1989**, *154*, 439−442.
(45) Noréus, D.; Törnroos, K. W.; Börje, A.; Szabò, T.; Bronger, W.; Spittank, H.; Auffermann, G.; Müller, P. *J. Less-Common Met* **1988**, *139*, 233−239.
(46) Bronger, W.; Auffermann, G. *J. Alloys Compd.* **1992**, *187*, 87−93.
(47) Bronger, W.; Brassard, L. à. *Z. Anorg. Allg. Chem.* **1996**, *622*, 462−464.
(48) Liao, M.-S.; Zhang, Q.-E.; Schwarz, W. H. E. *Z. Anorg. Allg. Chem.* **1998**, *624*, 1419−1428.
(49) Martínez-Coronado, R.; Retuerto, M.; Torres, B.; Martínez-Lope, M. J.; Fernández-Díaz, M. T.; Alonso, J. A. *Int. J. Hydrogen Energy* **2013**, *38*, 5738−5745.
(50) Jiang, J.; Zhang, S.; Huang, S.; Wang, P.; Tian, H. *Comput. Mater. Sci.* **2013**, *74*, 55−64.
(51) Polanski, M.; Nielsen, T. K.; Kunce, I.; Norek, M.; Płociński, T.; Jaroszewicz, L. R.; Gundlach, C.; Jensen, T. R.; Bystrzycki, J. *Int. J. Hydrogen Energy* **2013**, *38*, 4003−4010.